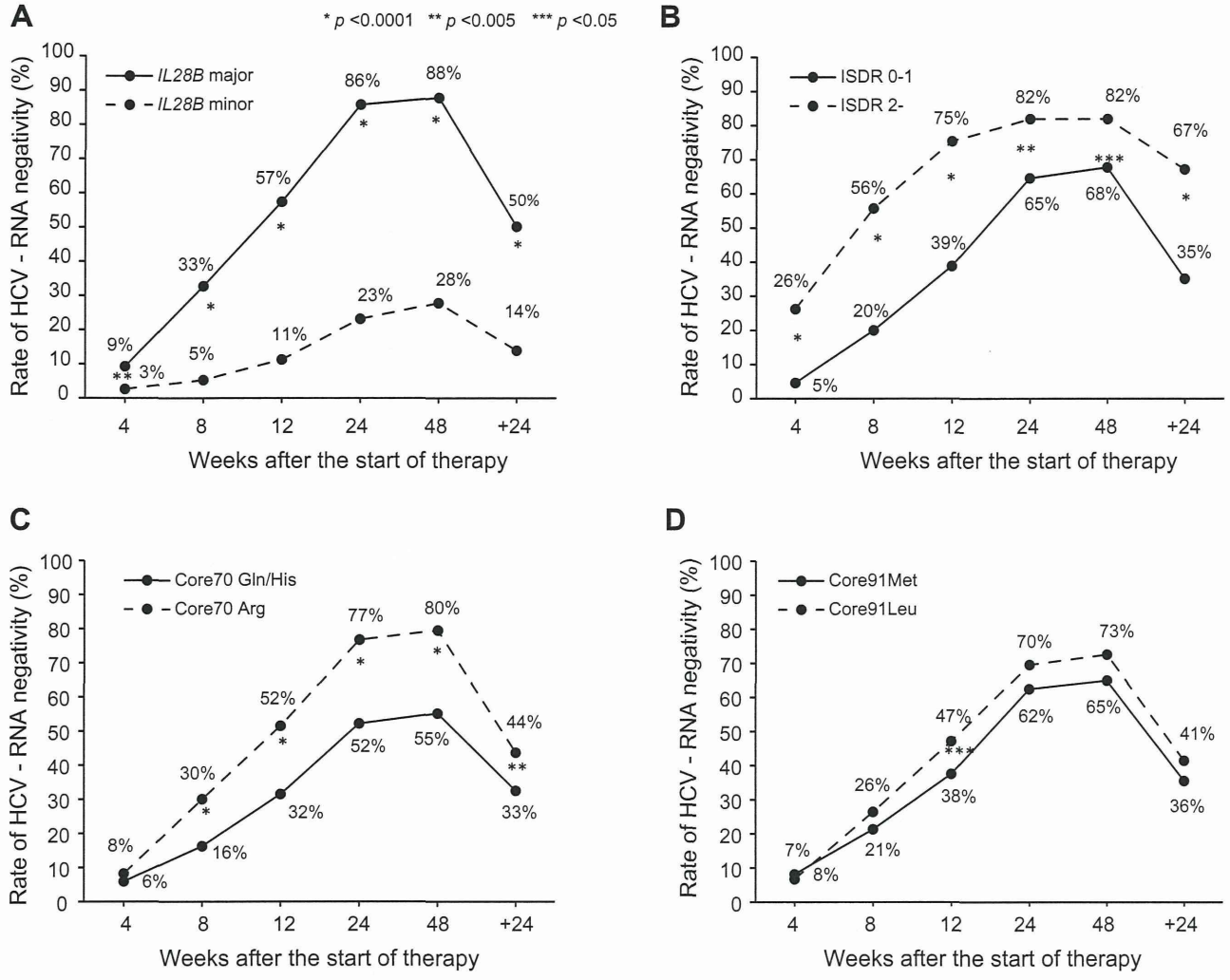

Fig. 2. Effect of *IL28B* mutations in the ISDR, Core70, and Core91 of HCV on time-dependent clearance of HCV. The rate of undetectable HCV-RNA was plotted for serial time points after the start of therapy (4, 8, 12, 24, and 48 weeks) and for 24 weeks after the completion of therapy. Patients were stratified according to (A) the *IL28B* allele (minor allele vs. major allele), (B) the number of mutations in the ISDR (0–1 mutation vs. 2 or more mutations), amino acid substitutions of (C) Core70 (Gln/His vs. Arg), and (D) Core91 (Met vs. Leu). The *p* values are from Fisher's exact test.

HCV-RNA ($p = 0.035$), Gln or His at Core70 ($p < 0.0001$), low platelet counts ($p = 0.009$), and advanced fibrosis ($p = 0.0002$) were associated with NVR. By multivariate analysis, the minor allele of *IL28B* (OR = 20.83, 95%CI = 11.63–37.04, $p < 0.0001$) was associated with NVR independent of other covariates (Table 2). Notably, mutations in the ISDR ($p = 0.707$) and at amino acid Core70 ($p = 0.207$) were not significant in multivariate analysis due to the positive correlation with the *IL28B* polymorphism ($p = 0.004$ for ISDR and $p < 0.0001$ for Core70, Fig. 4).

Genetic polymorphism of *IL28B* also was associated with SVR (OR = 7.41, 95% CI = 4.05–13.57, $p < 0.0001$) independent of other covariates, such as platelet counts, fibrosis, and serum levels of HCV-RNA. Mutation in the ISDR was an independent predictor of SVR (OR = 2.11, 95% CI = 1.06–4.18, $p = 0.033$) but the amino acid at Core70 was not (Table 3).

Factors associated with the IL28B polymorphism

Patients with the *IL28B* minor allele had significantly higher serum level of gamma-glutamyltransferase (GGT) and a higher frequency of hepatic steatosis (Table 4). When the association between the *IL28B* polymorphism and HCV sequences was analyzed, Gln or His at Core70, that is linked to resistance to PEG-IFN and RBV therapy [4,14,15], was significantly more frequent in patients with the minor *IL28B* allele than in those with the major allele (67% vs. 30%, $p < 0.0001$) (Fig. 4). Other HCV sequences with an IFN resistant phenotype also were more prevalent in patients with the minor *IL28B* allele than those with the major allele: Met at Core91 (46% vs. 37%, $p = 0.047$) and one or no mutations in the ISDR (94% vs. 85%, $p = 0.004$) (Fig. 4).

Data mining analysis

Data mining analysis was performed to build a model for the prediction of SVR and the result is shown in Fig. 5. The analysis selected four predictive variables, resulting in six subgroups of patients. Genetic polymorphism of *IL28B* was selected as the best predictor of SVR. Patients with the minor *IL28B* allele had a lower probability of SVR and a higher probability of NVR than those with the major *IL28B* allele (SVR: 14% vs. 50%, NVR: 72% vs.

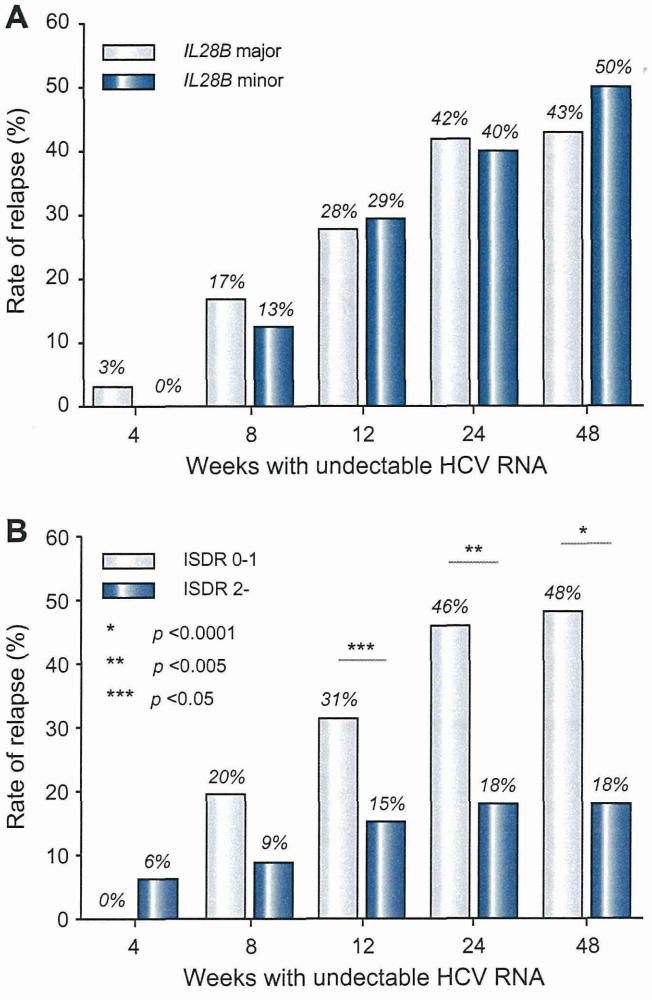

Fig. 3. Association between relapse and the *IL28B* allele or mutations in the ISDR. The rate of relapse was calculated for patients who had undetectable HCV-RNA at serial time points after the start of therapy (4, 8, 12, 24, and 48 weeks). Patients were stratified according to (A) the *IL28B* allele (minor allele vs. major allele) and (B) the number of mutations in the ISDR (0–1 mutation vs. 2 or more mutations). The *p* values are from Fisher's exact test.

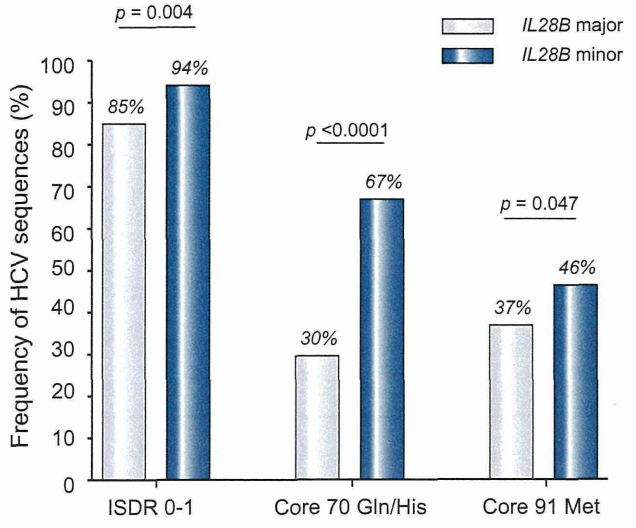

Fig. 4. Associations between the *IL28B* allele and HCV sequences. The prevalence of HCV sequences predicting a resistant phenotype to IFN was higher in patients with the minor *IL28B* allele than those with major allele. (A) 0 or 1 mutation in the ISDR of NS5A, (B) Gln or His at Core70, and (C) Met at Core91. *p* values are from Fisher's exact test.

12%). After stratification by the *IL28B* allele, patients with low platelet counts (<140 $\times$ 10^9/L) had a lower probability of SVR and higher probability of NVR than those with high platelet counts ($\geqslant$140 $\times$ 10^9/L): for the minor *IL28B* allele, SVR was 7% vs. 19%, and NVR was 84% vs. 62%, and for the major *IL28B* allele, SVR was 32% vs. 66% and NVR was 16% vs. 8%. Among patients with the major *IL28B* allele and low platelet counts, those with two or more mutations in the ISDR had a higher probability of SVR and lower probability of relapse than those with one or no mutations in the ISDR (SVR: 75% vs. 27%, and relapse: 8% vs. 57%). Among patients with the major *IL28B* allele and high platelet counts, those with a low HCV-RNA titer (<600,000 IU/ml) had a higher probability of SVR and lower probability of NVR and relapse than those with a high HCV-RNA titer (SVR: 90% vs. 61%, NVR: 0% vs. 10%, and relapse: 10% vs. 29%). The sensitivity and specificity of the decision tree were 78% and 70%, respectively. The area under the receiver operating characteristic (ROC) curve of the model was 0.782 (data not shown). The proportion of patients with advanced fibrosis (F3-4) was 39% (84/217) in patients with low platelet counts (<140 $\times$ 10^9/L) compared to 13% (37/279) in those with high platelet counts ($\geqslant$140 $\times$ 10^9/L).

Validation of the data mining analysis

The results of the data mining analysis were validated with 165 patients who differed from those used for model building. Each patient was allocated to one of the six subgroups for the validation using the flow-chart form of the decision tree. The rate of SVR and NVR in each subgroup was calculated. The rates of SVR and NVR for each subgroup of patients were closely correlated between the model building and the validation patients (r^2 = 0.99 and 0.98) (Fig. 6).

Discussion

The rate of NVR after 48 weeks of PEG-IFN/RBV therapy among patients infected with HCV of genotype 1 is around 20–30%. Previously, there have been no reliable baseline predictors of NVR or SVR. Because more potent therapies, such as protease and polymerase inhibitor of HCV [28,29] and nitazoxanide [30], are in clinical trials and may become available in the near future, a pre-treatment prediction of the likelihood of response may be helpful for patients and physicians, to support clinical decisions about whether to begin the current standard of care or whether to wait for emerging therapies. This study revealed that the *IL28B* polymorphism was the overwhelming predictor of NVR and is independent of host factors and viral sequences reported previously. The *IL28B* encodes a protein also known as IFN-lambda 3, which is thought to suppress the replication of various viruses including HCV [31,32]. The results of the current study and the findings of the GWAS studies [6–9] may provide the rationale for developing diagnostic testing or an IFN-lambda based therapy for chronic hepatitis C in the future.

Table 2. Factors associated with NVR analyzed by univariate and multivariate logistic regression analysis.

	Univariate			Multivariate		
	Odds ratio	95%CI	*p* value	Odds ratio	95%CI	*p* value
Gender: female	0.98	0.67-1.45	0.938	1.29	0.75-2.23	0.363
Age	1.01	0.97-1.01	0.223	0.99	0.97-1.02	0.679
ALT	1.00	1.00-1.00	0.867	1.00	0.99-1.00	0.580
GGT	1.004	1.00-1.01	0.029	1.00	1.00-1.00	0.715
Platelets	0.95	0.91-0.99	0.009	0.92	0.87-0.98	0.006
Fibrosis: F3-4	2.23	1.46-3.42	0.0002	1.97	1.09-3.57	0.025
HCV-RNA: ≥600,000 IU/ml	1.83	1.05-3.19	0.035	2.49	1.17-5.29	0.018
ISDR mutation: ≤1	2.14	1.08-4.22	0.030	0.96	0.78-1.18	0.707
Core 70 (Gln/His)	3.23	2.16-4.78	<0.0001	1.41	0.83-2.42	0.207
Core 91 (Met)	1.39	0.95-2.06	0.093	1.21	0.72-2.04	0.462
IL28B: Minor allele	19.24	11.87-31.18	<0.0001	20.83	11.63-37.04	<0.0001

ALT, alanine aminotransferase; GGT, gamma-glutamyltransferase; ISDR, interferon sensitivity determining region; Gln, glutamine; His, histidine; Met, methionine; Minor allele, heterozygote or homozygote of minor allele.

Table 3. Factors associated with SVR analyzed by univariate and multivariate logistic regression analysis.

	Univariate			Multivariate		
	Odds ratio	95%CI	*p* value	Odds ratio	95%CI	*p* value
Gender: female	0.81	0.56-1.16	0.253	0.86	0.55-1.35	0.508
Age	0.97	0.95-0.99	0.0003	0.99	0.96-1.01	0.199
ALT	1.00	1.00-1.00	0.337	1.00	1.00-1.01	0.108
GGT	1.00	1.00-1.00	0.273	1.00	1.00-1.00	0.797
Platelets	1.12	1.01-116	<0.0001	1.13	1.08-1.19	<0.0001
Fibrosis: F0-2	2.64	1.65-4.22	<0.0001	1.87	1.07-3.28	0.029
HCV-RNA: <600,000 IU/ml	2.49	1.55-3.98	0.0001	2.75	1.55-4.90	0.001
ISDR mutation: 2≤	3.78	2.14-6.68	<0.0001	2.11	1.06-4.18	0.033
Core 70 (Arg)	1.61	1.11-2.28	0.012	0.84	0.52-1.35	0.470
Core 91 (Leu)	1.28	0.88-1.85	0.185	1.26	0.81-1.96	0.300
IL28B: Major allele	6.21	3.75-10.31	<0.0001	7.41	4.05-13.57	<0.0001

ALT, alanine aminotransferase; GGT, Gamma-glutamyltransferase; ISDR, interferon sensitivity determining region; Arg, arginine; Leu, leucine; Major allele, homozygote of major allele.

Among baseline factors, *IL28B* was the most significant predictor of NVR and SVR. Moreover, the *IL28B* allele type was also correlated with early virological response: the rate of RVR and cEVR was significantly high for the *IL28B* major allele compared to the *IL28B* minor allele: 9% vs. 3% for RVR and 57% vs. 11% for cEVR (Fig. 2). On the other hand, the relapse rate was not different between the *IL28B* genotypes within patients who achieved RVR or cEVR (Fig. 3). We believe that optimal therapy should be based on baseline features and a response-guided approach. Our findings suggest that the *IL28B* genotype is a useful baseline predictor of virological response which should be used for selecting the treatment regimen: whether to treat patients with PEG-IFN and RBV or to wait for more effective future therapy including direct acting antiviral drugs. On the other hand, baseline *IL28B* genotype might not be suitable for determining the treatment duration in patients who started PEG-IFN/RBV therapy and whose virological response is determined because the *IL28B* genotype is not useful for the prediction of relapse. The duration of therapy should be personalized based on the virological response. Future studies need to explore whether the combination of baseline *IL28B* genotype and response-guided approach further improves the optimization of treatment duration.

The SVR rate in patients having the *IL28B* minor allele was 14% in the present study while it was 23% in Caucasians and 9% in African Americans in a study by McCarthy et al. [33]. On the other hand, the SVR rate in patients having the *IL28B* minor allele was 28% in genotypes 1/4 compared to 80% in genotypes 2/3 in a study by Rauch et al. [9]. These data imply that the impact of the *IL28B* polymorphism on response to therapy may be different in terms of race, geographical areas, or HCV genotypes, and that our data need to be validated in future studies including different populations and geographical areas before generalization.

Table 4. Factors associated with IL28B genotype.

	IL28B major allele n = 345	*IL28B* minor allele n = 151	*p* value
Gender: male	166 (48%)	84 (56%)	0.143
Age (years)	57 ± 10	57 ± 10	0.585
ALT (IU/L)	79 ± 60	78 ± 62	0.842
Platelets (10^9/L)	153 ± 54	155 ± 52	0.761
GGT (IU/L)	51 ± 45	78 ± 91	0.001
Fibrosis: F3-4	76 (22%)	45 (30%)	0.063
Steatosis:			
>10%	16/88 (18%)	13/23 (57%)	0.024
>30%	6/88 (7%)	6/23 (26%)	0.017
HCV-RNA: >600,000 IU/ml	284 (82%)	125 (83%)	1.000

ALT, alanine aminotransferase; GGT, gamma-glutamyltransferase.

Four GWAS studies have shown the association between a genetic polymorphism near the *IL28B* gene and response to PEG-IFN plus RBV therapy. The SNPs that showed significant association with response were rs12979860 [8] and rs8099917 [6,7,9]. There is a strong linkage-disequilibrium (LD) between these two SNPs as well as several other SNPs near the *IL28B* gene in Japanese patients [34] but the degree of LD was weaker in Caucasians and Hispanics [8]. Thus, the combination of SNPs is not useful for predicting response in Japanese patients but may improve the predictive value in patients other than Japanese who have weaker LD between SNPs.

Other significant predictors of response independent of *IL28B* genotype were platelet counts, stage of fibrosis, and HCV RVA load. A previous study reported that platelet count is a predictor of response to therapy [35], and the lower platelet count was related with advanced liver fibrosis in the present study. The association between response to therapy and advanced fibrosis independent of the *IL28B* polymorphism is consistent with a recent study by Rauch et al. [9].

There is agreement that the viral genotype is significantly associated with the treatment outcome. Moreover, viral factors such as substitutions in the ISDR of the NS5A region [10] or in the amino acid sequence of the HCV core [4] have been studied in relation to the response to IFN treatment. The amino acid Gln or His at Core70 and Met at Core91 are repeatedly reported to be associated with resistance to therapy [4,14,15] in Japanese patients but these data wait to be validated in different populations or other geographical areas. In this study, we confirmed that patients with two or more mutations in the ISDR had a higher rate of undetectable HCV-RNA at each time point during therapy. In addition, the rate of relapse among patients who achieved cEVR was significantly lower in patients with two or more mutations in ISDR compared to those with only one or no mutations (15% vs. 31%, p <0.05). Thus, the ISDR sequence may be used to predict a relapse among patients who achieved virological response during therapy, while the *IL28B* polymorphism may be used to predict the virological response before therapy. A higher number of mutations in the ISDR are reported to have close association with SVR in Japanese [11–13,15,36] or Asian [37,38] populations but data from Western countries have been controversial [39–42]. A meta-analysis of 1230 patients including 525 patients from Europe has shown that there was a positive correlation between the SVR and the number of mutations in the ISDR in Japanese as well as in European patients [43] but this correlation was more pronounced in Japanese patients. Thus, geographical factors may account for the different impact of ISDR on treatment response, which may be a potential limitation of our study.

To our surprise, these HCV sequences were associated with the *IL28B* genotype: HCV sequences with an IFN resistant phenotype were more prevalent in patients with the minor IL28B allele than those with the major allele. This was an unexpected finding, as we initially thought that host genetics and viral sequences were completely independent. A recent study reported that the *IL28B* polymorphism (rs12979860) was significantly associated with HCV genotype: the *IL28B* minor allele was more frequent in HCV genotype 1-infected patients compared to patients infected with HCV genotype 2 or 3 [33]. Again, patients with the *IL28B* minor allele (IFN resistant genotype) were infected with HCV sequences that are linked to an IFN resistant phenotype. The mechanism for this association is unclear, but may be related to an interaction between the *IL28B* genotype and HCV sequences in the development of chronic HCV infection as discussed by McCarthy et al., since the *IL28B* polymorphism was associated with the natural clearance of HCV [44]. Alternatively, the HCV sequence within the patient may be selected during the course of chronic infection [45,46]. These hypotheses should be explored through prospective studies of spontaneous HCV clearance or by testing the time-dependent changes in the HCV sequence during the course of chronic infection.

How these host and viral factors can be integrated to predict the response to therapy in future clinical practice is an important question. Because various host and viral factors interact in the same patient, predictive analysis should consider these factors in combination. Using the data mining analysis, we constructed a simple decision tree model for the pre-treatment prediction of SVR and NVR to PEG-IFN/RBV therapy. The classification of patients based on the genetic polymorphism of *IL28B*, mutation in the ISDR, serum levels of HCV-RNA, and platelet counts, identified subgroups of patients who have the lowest probabilities of NVR (0%) with the highest probabilities of SVR (90%) as well as those who have the highest probabilities of NVR (84%) with the lowest probability of SVR (7%). The reproducibility of the model was confirmed by the independent validation based on a second group of patients. Using this model, we can rapidly develop an

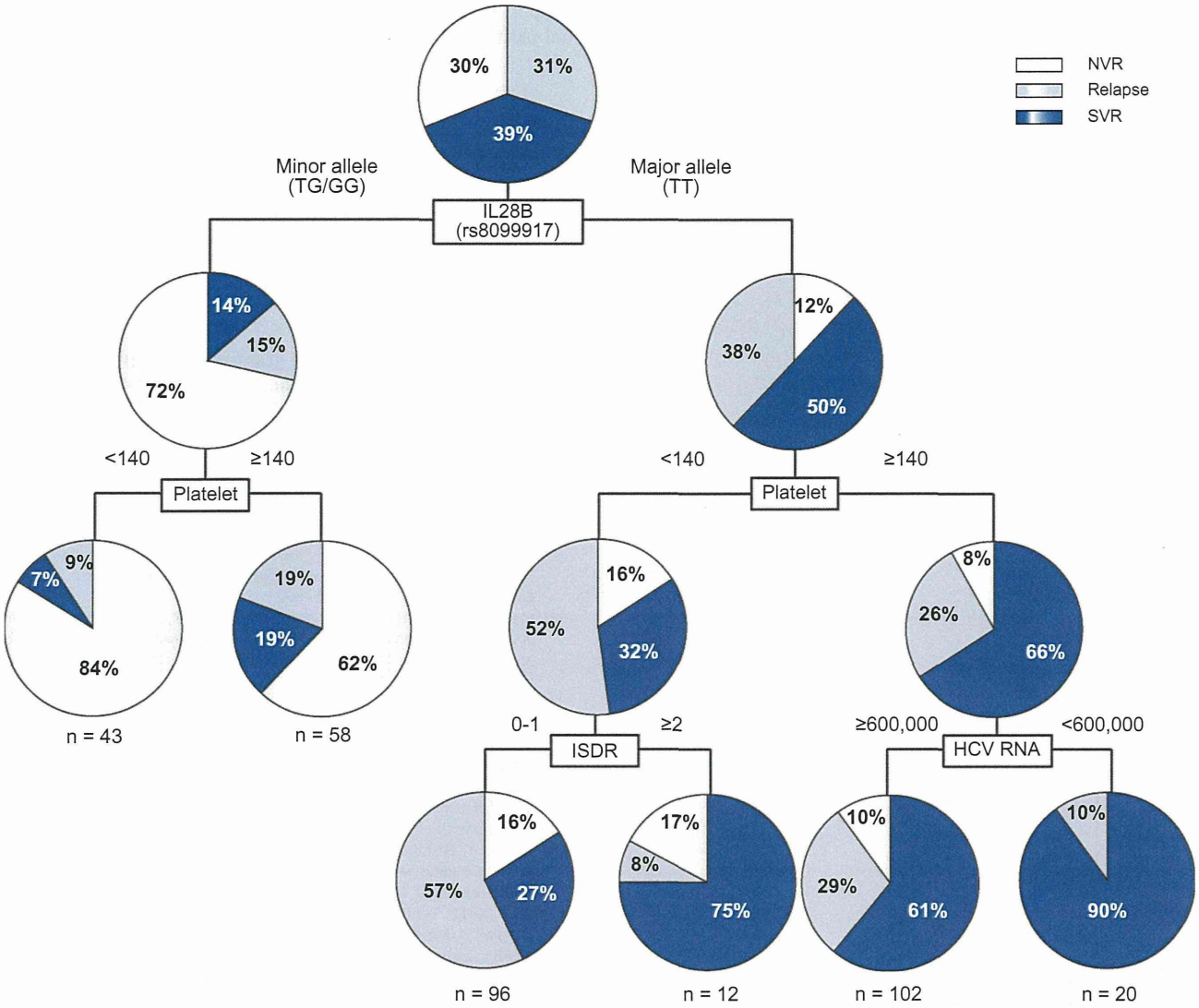

Fig. 5. Decision tree for the prediction of response to therapy. The boxes indicate the factors used for splitting. Pie charts indicate the rate of response for each group of patients after splitting. The rate of null virological response, relapse, and sustained virological response is shown.

estimate of the response before treatment, by simply allocating patients to subgroups by following the flow-chart form, which may facilitate clinical decision making. This is in contrast to the calculating formula, which was constructed by the traditional logistic regression model. This was not widely used in clinical practice as it is abstruse and inconvenient. These results support the evidence based approach of selecting the optimum treatment strategy for individual patients, such as treating patients with a low probability of NVR with current PEG-IFN/RBV combination therapy or advising those with a high probability of NVR to wait for more effective future therapies. Patients with a high probability of relapse may be treated for a longer duration to avoid a relapse. Decisions may be based on the possibility of a response against a potential risk of adverse events and the cost of the therapy, or disease progression while waiting for future therapy.

We have previously reported the predictive model of early virological response to PEG-IFN and RBV in chronic hepatitis C [26]. The top factor selected as significant was the grade of steatosis, followed by serum level of LDL cholesterol, age, GGT, and blood sugar. The mechanism of association between these factors and treatment response was not clear at that time. To our interest, a recent study by Li et al. [47] has shown that high serum level of LDL cholesterol was linked to the *IL28B* major allele (CC in rs12979860). High serum level of LDL cholesterol was associated with SVR but it was no longer significant when analyzed together with the *IL28B* genotype in multivariate analysis. Thus, the association between treatment response and LDL cholesterol levels may reflect the underlining link of LDL cholesterol levels to *IL28B* genotype. Steatosis is reported to be correlated with low lipid levels [48] which suggest that *IL28B* genotypes may be also associated with steatosis. In fact, there were significant correlations between the *IL28B* genotype and the presence of steatosis in the present study (Table 4). In addition, the serum level of GGT, another predictive factor in our previous study, was signif-

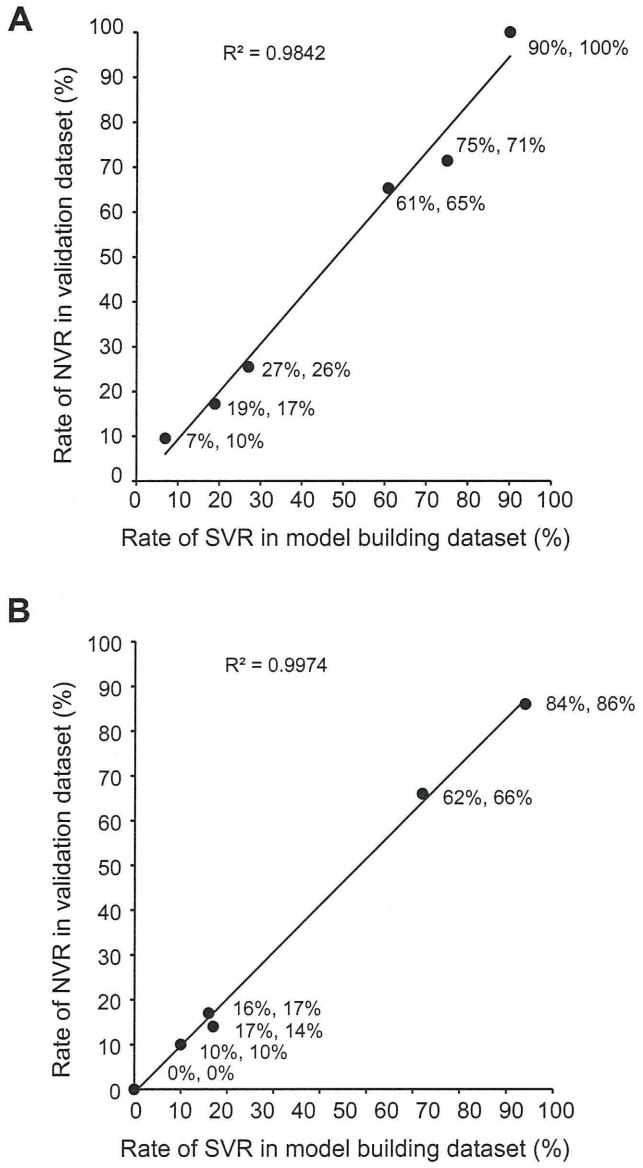

Fig. 6. Validation of the CART analysis. Each patient in the validation group was allocated to one of the six subgroups by following the flow-chart form of the decision tree. The rate of (A) sustained virological response (SVR) and (B) null virological response (NVR) in each subgroup was calculated and plotted. The *X*-axis represents the rate of SVR or NVR in the model building patients and the *Y*-axis represents those in the validation patients. The rate of SVR and NVR in each subgroup of patients is closely correlated between the model building and the validation patients (correlation coefficient: $r^2 = 0.98–0.99$).

icantly associated with *IL28B* genotype in the present study (Table 4). The serum level of GGT was significantly associated with NVR when examined independently but was no longer significant when analyzed together with the *IL28B* genotype. These observations indicate that some of the factors that we have previously identified may be associated with virological response to therapy through the underlining link to the *IL28B* genotype.

In conclusion, the present study highlighted the impact of the *IL28B* polymorphism and mutation in the ISDR on the pre-treatment prediction of response to PEG-IFN/RBV therapy. A decision model including these host and viral factors has the potential to support selection of the optimum treatment strategy for individual patients, which may enable personalized treatment.

Conflict of interest

The authors who have taken part in this study declare that they do not have anything to disclose regarding funding or conflict of interest with respect to this manuscript.

Financial support

This study was supported by a grant-in-aid from the Ministry of Health, Labor and Welfare, Japan, (H19-kannen-013), (H20-kannen-006).

References

[1] Ray Kim W. Global epidemiology and burden of hepatitis C. Microbes Infect 2002;4 (12):1219–1225.
[2] Fried MW, Shiffman ML, Reddy KR, Smith C, Marinos G, Goncales Jr FL, et al. Peginterferon alfa-2a plus ribavirin for chronic hepatitis C virus infection. N Engl J Med 2002;347 (13):975–982.
[3] Manns MP, McHutchison JG, Gordon SC, Rustgi VK, Shiffman M, Reindollar R, et al. Peginterferon alfa-2b plus ribavirin compared with interferon alfa-2b plus ribavirin for initial treatment of chronic hepatitis C: a randomised trial. Lancet 2001;358 (9286):958–965.
[4] Akuta N, Suzuki F, Sezaki H, Suzuki Y, Hosaka T, Someya T, et al. Association of amino acid substitution pattern in core protein of hepatitis C virus genotype 1b high viral load and non-virological response to interferon-ribavirin combination therapy. Intervirology 2005;48 (6):372–380.
[5] Davis GL, Wong JB, McHutchison JG, Manns MP, Harvey J, Albrecht J. Early virologic response to treatment with peginterferon alfa-2b plus ribavirin in patients with chronic hepatitis C. Hepatology 2003;38 (3):645–652.
[6] Tanaka Y, Nishida N, Sugiyama M, Kurosaki M, Matsuura K, Sakamoto N, et al. Genome-wide association of IL28B with response to pegylated interferon-alpha and ribavirin therapy for chronic hepatitis C. Nat Genet 2009;10:1105–1109.
[7] Suppiah V, Moldovan M, Ahlenstiel G, Berg T, Weltman M, Abate ML, et al. IL28B is associated with response to chronic hepatitis C interferon-alpha and ribavirin therapy. Nat Genet 2009;10:1100–1104.
[8] Ge D, Fellay J, Thompson AJ, Simon JS, Shianna KV, Urban TJ, et al. Genetic variation in IL28B predicts hepatitis C treatment-induced viral clearance. Nature 2009;461 (7262):399–401.
[9] Rauch A, Kutalik Z, Descombes P, Cai T, Di Iulio J, Mueller T, et al. Genetic variation in IL28B is associated with chronic hepatitis C and treatment failure: a genome-wide association study. Gastroenterology 2010;138 (4):1338–1345.
[10] Enomoto N, Sakuma I, Asahina Y, Kurosaki M, Murakami T, Yamamoto C, et al. Comparison of full-length sequences of interferon-sensitive and resistant hepatitis C virus 1b. Sensitivity to interferon is conferred by amino acid substitutions in the NS5A region. J Clin Invest 1995;96 (1):224–230.
[11] Enomoto N, Sakuma I, Asahina Y, Kurosaki M, Murakami T, Yamamoto C, et al. Mutations in the nonstructural protein 5A gene and response to interferon in patients with chronic hepatitis C virus 1b infection. N Engl J Med 1996;334 (2):77–81.
[12] Kurosaki M, Enomoto N, Murakami T, Sakuma I, Asahina Y, Yamamoto C, et al. Analysis of genotypes and amino acid residues 2209 to 2248 of the NS5A region of hepatitis C virus in relation to the response to interferon-beta therapy. Hepatology 1997;25 (3):750–753.
[13] Shirakawa H, Matsumoto A, Joshita S, Komatsu M, Tanaka N, Umemura T, et al. Pretreatment prediction of virological response to peginterferon plus ribavirin therapy in chronic hepatitis C patients using viral and host factors. Hepatology 2008;48 (6):1753–1760.
[14] Akuta N, Suzuki F, Kawamura Y, Yatsuji H, Sezaki H, Suzuki Y, et al. Predictive factors of early and sustained responses to peginterferon plus ribavirin combination therapy in Japanese patients infected with hepatitis C virus genotype 1b: amino acid substitutions in the core region and low-density lipoprotein cholesterol levels. J Hepatol 2007;46 (3):403–410.

[15] Okanoue T, Itoh Y, Hashimoto H, Yasui K, Minami M, Takehara T, et al. Predictive values of amino acid sequences of the core and NS5A regions in antiviral therapy for hepatitis C: a Japanese multi-center study. J Gastroenterol 2009;44 (9):952–963.
[16] Segal MR, Bloch DA. A comparison of estimated proportional hazards models and regression trees. Stat Med 1989;8 (5):539–550.
[17] LeBlanc M, Crowley J. A review of tree-based prognostic models. Cancer Treat Res 1995;75:113–124.
[18] Garzotto M, Beer TM, Hudson RG, Peters L, Hsieh YC, Barrera E, et al. Improved detection of prostate cancer using classification and regression tree analysis. J Clin Oncol 2005;23 (19):4322–4329.
[19] Averbook BJ, Fu P, Rao JS, Mansour EG. A long-term analysis of 1018 patients with melanoma by classic Cox regression and tree-structured survival analysis at a major referral center: implications on the future of cancer staging. Surgery 2002;132 (4):589–602.
[20] Leiter U, Buettner PG, Eigentler TK, Garbe C. Prognostic factors of thin cutaneous melanoma: an analysis of the central malignant melanoma registry of the german dermatological society. J Clin Oncol 2004;22 (18):3660–3667.
[21] Valera VA, Walter BA, Yokoyama N, Koyama Y, Iiai T, Okamoto H, et al. Prognostic groups in colorectal carcinoma patients based on tumor cell proliferation and classification and regression tree (CART) survival analysis. Ann Surg Oncol 2007;14 (1):34–40.
[22] Zlobec I, Steele R, Nigam N, Compton CC. A predictive model of rectal tumor response to preoperative radiotherapy using classification and regression tree methods. Clin Cancer Res 2005;11 (15):5440–5443.
[23] Thabane M, Simunovic M, Akhtar-Danesh N, Marshall JK. Development and validation of a risk score for post-infectious irritable bowel syndrome. Am J Gastroenterol 2009;104 (9):2267–2274.
[24] Wu BU, Johannes RS, Sun X, Tabak Y, Conwell DL, Banks PA. The early prediction of mortality in acute pancreatitis: a large population-based study. Gut 2008;57 (12):1698–1703.
[25] Fonarow GC, Adams Jr KF, Abraham WT, Yancy CW, Boscardin WJ. Risk stratification for in-hospital mortality in acutely decompensated heart failure: classification and regression tree analysis. Jama 2005;293 (5):572–580.
[26] Kurosaki M, Matsunaga K, Hirayama I, Tanaka T, Sato M, Yasui Y, et al. A predictive model of response to peginterferon ribavirin in chronic hepatitis C using classification and regression tree analysis. Hepatol Res 2010;40 (3):251–260.
[27] Nishida N, Tanabe T, Takasu M, Suyama A, Tokunaga K. Further development of multiplex single nucleotide polymorphism typing method, the DigiTag2 assay. Anal Biochem 2007;364 (1):78–85.
[28] Hezode C, Forestier N, Dusheiko G, Ferenci P, Pol S, Goeser T, et al. Telaprevir and peginterferon with or without ribavirin for chronic HCV infection. N Engl J Med 2009;360 (18):1839–1850.
[29] McHutchison JG, Everson GT, Gordon SC, Jacobson IM, Sulkowski M, Kauffman R, et al. Telaprevir with peginterferon and ribavirin for chronic HCV genotype 1 infection. N Engl J Med 2009;360 (18):1827–1838.
[30] Rossignol JF, Elfert A, El-Gohary Y, Keeffe EB. Improved virologic response in chronic hepatitis C genotype 4 treated with nitazoxanide, peginterferon, and ribavirin. Gastroenterology 2009;136 (3):856–862.
[31] Marcello T, Grakoui A, Barba-Spaeth G, Machlin ES, Kotenko SV, MacDonald MR, et al. Interferons alpha and lambda inhibit hepatitis C virus replication with distinct signal transduction and gene regulation kinetics. Gastroenterology 2006;131 (6):1887–1898.
[32] Robek MD, Boyd BS, Chisari FV. Lambda interferon inhibits hepatitis B and C virus replication. J Virol 2005;79 (6):3851–3854.
[33] McCarthy JJ, Li JH, Thompson A, Suchindran S, Lao XQ, Patel K, et al. Replicated association between an IL28B Gene Variant and a Sustained Response to Pegylated Interferon and Ribavirin. Gastroenterology 2010;138:2307–2314.
[34] Tanaka Y, Nishida N, Sugiyama M, Tokunaga K, Mizokami M. Λ-interferons and the single nucleotide polymorphisms: a milestone to tailor-made therapy for chronic hepatitis C. Hepatol Res 2010;40:449–460.
[35] Backus LI, Boothroyd DB, Phillips BR, Mole LA. Predictors of response of US veterans to treatment for the hepatitis C virus. Hepatology 2007;46 (1):37–47.
[36] Mori N, Imamura M, Kawakami Y, Saneto H, Kawaoka T, Takaki S, et al. Randomized trial of high-dose interferon-alpha-2b combined with ribavirin in patients with chronic hepatitis C: correlation between amino acid substitutions in the core/NS5A region and virological response to interferon therapy. J Med Virol 2009;81 (4):640–649.
[37] Hung CH, Lee CM, Lu SN, Lee JF, Wang JH, Tung HD, et al. Mutations in the NS5A and E2-PePHD region of hepatitis C virus type 1b and correlation with the response to combination therapy with interferon and ribavirin. J Viral Hepat 2003;10 (2):87–94.
[38] Yen YH, Hung CH, Hu TH, Chen CH, Wu CM, Wang JH, et al. Mutations in the interferon sensitivity-determining region (nonstructural 5A amino acid 2209–2248) in patients with hepatitis C-1b infection and correlating response to combined therapy of pegylated interferon and ribavirin. Aliment Pharmacol Ther 2008;27 (1):72–79.
[39] Zeuzem S, Lee JH, Roth WK. Mutations in the nonstructural 5A gene of European hepatitis C virus isolates and response to interferon alfa. Hepatology 1997;25 (3):740–744.
[40] Squadrito G, Leone F, Sartori M, Nalpas B, Berthelot P, Raimondo G, et al. Mutations in the nonstructural 5A region of hepatitis C virus and response of chronic hepatitis C to interferon alfa. Gastroenterology 1997;113 (2):567–572.
[41] Sarrazin C, Berg T, Lee JH, Teuber G, Dietrich CF, Roth WK, et al. Improved correlation between multiple mutations within the NS5A region and virological response in European patients chronically infected with hepatitis C virus type 1b undergoing combination therapy. J Hepatol 1999;30 (6):1004–1013.
[42] Murphy MD, Rosen HR, Marousek GI, Chou S. Analysis of sequence configurations of the ISDR, PKR-binding domain, and V3 region as predictors of response to induction interferon-alpha and ribavirin therapy in chronic hepatitis C infection. Dig Dis Sci 2002;47 (6):1195–1205.
[43] Pascu M, Martus P, Hohne M, Wiedenmann B, Hopf U, Schreier E, et al. Sustained virological response in hepatitis C virus type 1b infected patients is predicted by the number of mutations within the NS5A-ISDR: a meta-analysis focused on geographical differences. Gut 2004;53 (9):1345–1351.
[44] Thomas DL, Thio CL, Martin MP, Qi Y, Ge D, O'Huigin C, et al. Genetic variation in IL28B and spontaneous clearance of hepatitis C virus. Nature 2009;461 (7265):798–801.
[45] Kurosaki M, Enomoto N, Marumo F, Sato C. Evolution and selection of hepatitis C virus variants in patients with chronic hepatitis C. Virology 1994;205 (1):161–169.
[46] Enomoto N, Kurosaki M, Tanaka Y, Marumo F, Sato C. Fluctuation of hepatitis C virus quasispecies in persistent infection and interferon treatment revealed by single-strand conformation polymorphism analysis. J Gen Virol 1994;75 (Pt 6):1361–1369.
[47] Li JH, Lao XQ, Tillmann HL, Rowell J, Patel K, Thompson A, et al. Interferon-lambda genotype and low serum low-density lipoprotein cholesterol levels in patients with chronic hepatitis C infection. Hepatology 1904;51 (6):1904–1911.
[48] Serfaty L, Andreani T, Giral P, Carbonell N, Chazouilleres O, Poupon R. Hepatitis C virus induced hypobetalipoproteinemia: a possible mechanism for steatosis in chronic hepatitis C. J Hepatol 2001;34 (3):428–434.

Hepatology Research

Hepatology Research 2011; **41**: 217–224 doi: 10.1111/j.1872-034X.2010.00768.x

Original Article

Changes in hepatitis C viral load during first 14 days can predict the undetectable time point of serum viral load by pegylated interferon and ribavirin therapy

Jun Itakura,[1] Yasuhiro Asahina,[1] Nobuharu Tamaki,[1] Itsuko Hirayama,[1] Yutaka Yasui,[1] Tomohiro Tanaka,[1] Mitsuaki Sato,[1] Ken Ueda,[1] Teiji Kuzuya,[1] Kaoru Tsuchiya,[1] Hiroyuki Nakanishi,[1] Masayuki Kurosaki,[1] Gretchen S. Gabriel,[2] George J. Schneider[2] and Namiki Izumi[1]

[1]*Division of Gastroenterology and Hepatology, Musashino Red Cross Hospital, Tokyo, Japan; and* [2]*Abbott Molecular, Des Plaines, Illinois, USA*

Aim: In the treatment of chronic hepatitis C, pegylated interferon (PEG-IFN) and ribavirin combination therapy must be continued for an adequate duration to improve the rate of sustained virological response. We attempted to predict the time point at which serum hepatitis C virus (HCV) RNA are undetectable during combination therapy.

Methods: Patients with HCV genotype 1b were enrolled in a model preparation ($n = 35$) and a validation group ($n = 70$). All patients received PEG-IFN-α-2b/ribavirin combination therapy for at least 48 weeks, and serological samples were screened a minimum of 17 times during the therapy. Serum HCV RNA were measured by the Abbott RealTime HCV assay. Using the HCV dynamics model described by Neumann *et al.*, we used multiple linear regression analysis to select factors that affected the undetectable time point.

Results: Difference in viral load between weeks 1 and 2 was the only predictive factor for the undetectable time point of serum HCV RNA ($r^2 = 0.67$, $P < 0.0005$), and we derived the following prediction equation: undetectable time point (week) = 13.495 × (viral load at day 14 [log IU/mL] – viral load at day 7 [log IU/mL]) + 25.456. The equation was applicable to the validation group.

Conclusion: We created a formula for predicting the undetectable time point from viral load measurements early in PEG-IFN-α-2b/ribavirin combination therapy. An early response reflects sensitivity to therapy, and the estimation of an undetectable time point would be useful for determining the optimal duration of treatment for chronic hepatitis C patients.

Key words: hepatitis C, interferon, kinetics, real-time polymerase chain reaction, undetectable time point

INTRODUCTION

INTERFERON (IFN)-BASED therapy is the main form of therapy for chronic hepatitis C, but it requires a long-term period to complete, typically lasting at least 48 weeks for hepatitis C virus (HCV) genotypes 1 and 4. The final therapeutic effect is eradication of HCV, which is referred to as a sustained virological response (SVR). Although combination therapy with pegylated (PEG)-IFN-α and ribavirin is now established as the standard treatment for chronic HCV infection genotype 1b, the SVR rate in these patients is still approximately 50%.[1–3] Moreover, it is difficult to know the treatment outcomes during treatment and follow-up period.

Various factors have been investigated to predict the treatment efficacy before initiation of therapy, including pretreatment viral load,[4] viral genotype,[5] and gene sequences, such as IFN sensitivity determining region,[6] and host factors, including sex, age, fibrosis stage and race.[7,8] These factors cannot be modified by therapy and are unfortunately not completely reliable for predicting therapeutic response. However, other studies have documented the importance of the period when HCV is cleared from the serum (we define this as the

Correspondence: Dr Namiki Izumi, Division of Gastroenterology and Hepatology, Musashino Red Cross Hospital, 1-26-1 Kyonan-cho, Musashino-shi, Tokyo 180-8610, Japan. Email: nizumi@musashino.jrc.or.jp

There are no conflicts of interests regarding this study.

Received 13 November 2009; revised 18 November 2010; accepted 18 December 2010.

"undetectable time point").[9–13] When an undetectable time point is achieved within 4 weeks of therapy initiation, the SVR rate is high. In contrast, the later the undetectable time point, the lower the SVR rate. One disadvantage with this prediction method during therapy is that SVR cannot be predicted until serum viral clearance. If one can predict the undetectable time point early during the treatment, physicians can modify and optimize the ongoing treatment.

There are various patterns of patient response to IFN therapy. In clinical settings, the following three response patterns are observed: (i) SVR; (ii) non-virological response (NVR), in which viral loads continue to be detected during therapy; and (iii) relapse, in which viral loads transiently drop below the detection limit but become detectable again after the end of therapy.[8] Mathematical models have been developed for analyzing therapy-induced changes in HCV viral load. Neumann *et al.*[14] introduced a model for IFN monotherapy in 1998, and a pharmacokinetic model for PEG-IFN has been developed by Powers *et al.*[15] These models are very useful for understanding the therapeutic effects of IFN on HCV.

In recent years, techniques to quantify serum viral RNA levels have advanced. The detection limit and the dynamic range of the quantitative real-time polymerase chain reaction (PCR) assay are lower and wider than those of Amplicor PCR assay.[16,17] As a result, the real-time PCR assay can show us the more accurate viral dynamics. In the present study, we used the model of Powers *et al.*[15] and real-time PCR to measure serum viral loads. Our aim was to ascertain whether it is possible to predict the undetectable time point during the early stage of PEG-IFN-α-2b/ribavirin combination therapy for genotype 1b patients with a high viral load, which is the most difficult-to-treat phenotype of HCV.

METHODS

Patients

THE MODEL PREPARATION group comprised 35 patients with biopsy-proven chronic hepatitis C who were treated at the Musashino Red Cross Hospital from 2000–2001. All patients had HCV genotype 1b and a high viral load (>100 000 IU/mL) as determined by the Amplicor-HCV Monitor Assay (Roche Diagnostics, Tokyo, Japan). Patients with other liver disease, such as liver cirrhosis, autoimmune hepatitis or alcoholic liver injury, were excluded. None of the patients had hepatitis B virus-related antigens, antibodies or anti-HIV antibodies. At the time of enrollment, it was confirmed that none of the patients were taking drugs that could affect their immune system. The dosage of ursodeoxycholic acid and glycyrrhizin was not changed during therapy.

The model validation group comprised 70 patients with biopsy-proven chronic hepatitis C who were treated at the Musashino Red Cross Hospital from 2004–2006. As with the model preparation group, all patients had HCV genotype 1b and a high viral load, and patients with liver cirrhosis or alcoholic liver injury were excluded. None of the patients had hepatitis B virus-related antigens, antibodies or anti-HIV antibodies.

Informed consent was obtained from all patients in writing. The present study was approved by the Ethics Review Board of Musashino Red Cross Hospital in accordance with the Declaration of Helsinki.

Treatment protocol

All patients received at least 48 weeks of PEG-IFN-α-2b (PegIntron; Schering-Plough, Kenilworth, NJ, USA) and ribavirin (Rebetol; Schering-Plough) combination therapy. In the model validation group, if viral clearance was not achieved by week 12, combination therapy was prolonged to 72 weeks. PEG-IFN-α-2b (1.5 μg/kg per week) was administrated s.c. Ribavirin was administrated p.o. at 600 mg/day twice daily to patients weighing less than 60 kg, and 800 mg/day was given to patients weighing between 60 and 80 kg. The dosage of PEG-IFN-α-2b was reduced to 0.75 μg/kg per week when white blood cells, neutrophils or platelets dropped below 1500, 750 or $80 \times 10^3/mm^3$, respectively. When hemoglobin concentration dropped below 10 g/dL, the dosage of ribavirin was reduced from 600 to 400 mg/day for patients weighing less than 60 kg, and from 800 to 600 mg/day for patients weighing between 60 and 80 kg. Both drugs were discontinued when white blood cells, neutrophils, platelets or hemoglobin levels dropped below $1000/mm^3$, $500/mm^3$, $50 \times 10^3/mm^3$ or 8.5 g/dL, respectively.

HCV dynamics in serum

To analyze viral dynamics, serum samples were collected from each patient according to the following schedule with respect to the start of PEG-IFN-α2b/ribavirin combination therapy: immediately before and at 4, 8 h, and 1, 2, 4, 7, 8, 14 and 28 days after the therapy was started; and then at 4-week intervals until completion of the therapy. HCV viral loads were measured in all serum samples using the Abbott RealTi*m*e HCV assay (Abbott Molecular, Des Plaines, IL, USA) at an Abbott laboratory in the USA.[16] The dynamic range

was 1.08–8 $\log_{10}$ IU/mL. The assay is standardized to the 2nd World Health Organization (WHO) International Standard for HCV RNA (National Institute for Biological Standards and Control code 96/798). Nucleic acid extraction was performed on 0.5-mL samples using an Abbott *m2000sp* (Abbott Molecular). The Abbott *m2000rt* (Abbott Molecular) was used for reverse transcription, PCR amplification and detection/quantification. A single-stranded linear probe was used as the HCV probe.

Definitions of response to therapy

The undetectable time point was defined as the first time the viral load dropped below the detection limit (1.08 $\log_{10}$ IU/mL) during therapy. Patients with SVR had no detectable viral load 6 months after the end of PEG-IFN-α-2b/ribavirin combination therapy. Patients in relapse had no detectable viral load at the end of therapy but had a detectable viral load 6 months after the end of therapy. Patients with NVR had a detectable viral load throughout the treatment period.

Calculation of the HCV dynamic parameters

Hepatitis C virus dynamic parameters (c, δ, ε, T_0 and V_0) were calculated from viral loads with equations for HCV dynamics.[15] The parameter c is the constant viral death rate, δ is the death rate of infected cells, ε is the effect of PEG-IFN on blocking production of virus from infected cells, and T_0 and V_0 are the numbers of uninfected cells and virus at the start of therapy, respectively.

Statistical analysis

SAS ver. 9.13 was used for the statistical analysis. *P*-values of less than 0.05 were considered significant.

RESULTS

Baseline patient characteristics

TABLE 1 SHOWS the baseline characteristics of the patients. The SVR rate was 60% and 27 patients accomplished undetectable serum HCV until 24 weeks after the therapy was started. The therapy was discontinued in three of the 35 patients because of a reduction in

Table 1 Patient characteristics at baseline

	Model preparation group ($n = 35$)	Model verification group ($n = 70$)
Age (years)	52.1 ± 9.9	57.8 ± 11
Sex (male/female)	24/11	36/34
BMI	23.7 ± 2.9	23.9 ± 3.7
Hemoglobin (g/dL)	14.7 ± 1.2	14.2 ± 1.6
Platelet count ($\times 10^3/\mu$L)	17.9 ± 4.8	15.5 ± 5.2
Albumin (g/dL)	4.2 ± 0.33	3.92 ± 0.048
ALT (U/L)	91.7 ± 64	80.0 ± 7.4
Liver histology (Metavir score)		
A (0/1/2/3/4/not measured)	0/17/13/5/0/0	0/40/26/2/0/2
F (0/1/2/3/4/not measured)	0/17/15/3/0/0	2/23/25/18/0/2
Viral load (log IU/mL)		
At pretreatment	5.49 ± 0.52	5.54 ± 0.92
At 7th day of treatment	4.05 ± 0.98	4.75 ± 1.05
at 14th day of treatment	3.23 ± 1.41	4.23 ± 1.29
Durations of therapy		
(48 weeks/72 weeks/dropout)	32/0/3	45/7/18
Drug adherence†		
(PEG-IFN/ribavirin/both/non-)	7/5/2/21	6/21/30/13
Outcome (SVR/relapse/NVR)	21/6/8	20/26/24
Actual undetectable time point‡		
(14/28 days/8/12/16/20/24/28/32 weeks/therapy end)	3/7/8/4/1/2/2/0/0	2/2/12/14/4/4/2/2/4

†Patients numbers with dose reduction during the therapy.
‡NVR cases were excluded.
BMI, body mass index; ALT, alanine aminotransferase; PEG-IFN, pegylated interferon; SVR, sustained virological response; NVR, non-virological response.

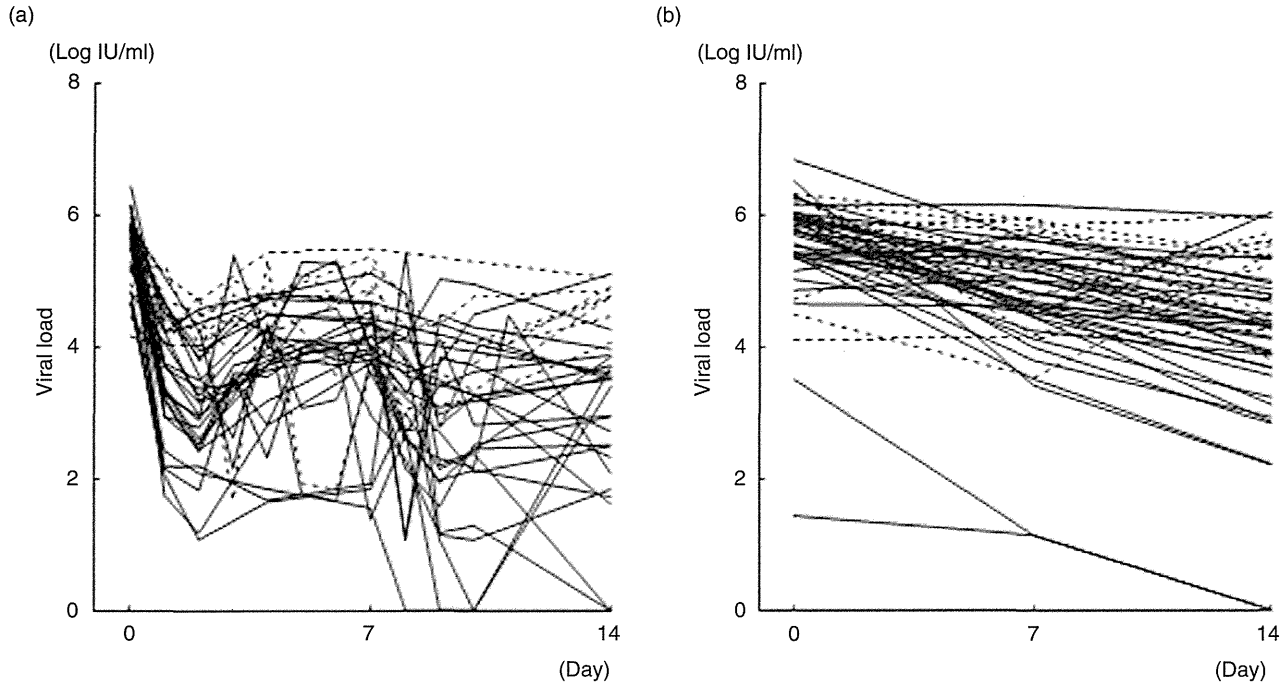

Figure 1 Early hepatitis C virus (HCV) dynamics of model preparation group (a) and of model validation group (b). The patients with incomplete blood collection were excluded from the figure of the model validation group. Solid line, dynamics of those who accomplished undetectable serum HCV until the therapy ended; dotted line, of those in whom serum HCV was detected through the whole therapy.

the hemoglobin concentration, a reduction in the neutrophil count and a worsening of depressive symptoms. In comparison to the model preparation group, there were more NVR patients, and the SVR rate was 29% in the model validation group. There were six patients who accomplished undetectable serum HCV after 24 weeks, and the latest patients achieved it 40 weeks after the therapy started. More patients had advanced hepatic fibrosis in the model validation group than in the model preparation group. Eighteen patients discontinued the combination therapy for various reasons, for example, decreased neutrophil count. The early HCV dynamics of both group are shown in Figure 1.

Undetectable time point prediction

From the model preparation group, 29 patients were analyzed and six patients were excluded for the following reasons: therapy was discontinued before viral clearance in one patient, PEG-IFN dosage was decreased before viral clearance in three patients, viral load increased during therapy in one patient, and an incomplete series of samples were obtained from one patient.

First, we hypothesized that the HCV dynamic parameters have a possibility to predict the undetectable time point. HCV dynamic parameters were calculated with three dataset patterns of viral loads, as follows: (i) immediately before and at 4, 8 h, and 1, 2, 4, 7 and 8 days; (ii) before and at 8 h, and 1, 2, 4 and 7 days; and (iii) before and at 4, 8 h, and 1, 2, 4 and 7 days after the therapy was started. Unfortunately, no significant factors for prediction of the undetectable time points were detected in these HCV dynamic parameters (Table 2), even when adding parameters of age and sex.

Next, we investigated the possibility using early-stage treatment dynamics. Multiple linear regression analysis was conducted for viral load, and changes in viral load up to day 14 as the explanatory variables and undetectable time points as the objective variables. Among various factors which became significant alone, the decrease in viral load from day 7 to 14 was found to be the best predictor for the undetectable time points by multiple linear regression analysis ($r^2 = 0.67$, Table 3). Then, whole datasets were analyzed again including HCV dynamic parameters, sex, age, viral loads and viral

Table 2 Calculated HCV-dynamic parameters of model preparation group

Dataset	Dataset 1† median (range)	*P*	Dataset 2‡ median (range)	*P*	Dataset 3§ median (range)	*P*
c	0.77 (0.032–5.21)	0.73	1.54 (0.0515–7.58)	0.37	2.75 (0.040–6.19)	0.85
δ	0.0033 (0–0.69)	0.76	0.013 (0–0.99)	0.094	0.053 (0–0.70)	0.91
ε	0.28 (0.023–0.84)	0.30	0.067 (0.0083–0.72)	0.038	0.28 (0.023–0.71)	0.18
T_0	0.36 (0.0001–0.95)	0.63	0.415 (0.0049–0.98)	0.23	0.36 (0.007–0.90)	0.21
V_0	5.49 (4.40–6.69)	0.53	4.99 (4.10–6.48)	0.090	5.29 (4.30–6.69)	0.29
R^2	0.012		0.090		0.056	

†Dataset 1: serum hepatitis C virus (HCV) load immediately before and at 4, 8 h, and 1, 2, 4, 7, 8 days after the therapy was started.
‡Dataset 2: serum HCV load before and at 8 h, and 1, 2, 4, 7 days after the therapy was started.
§Dataset 3: serum HCV load before and at 4, 8 h, and 1, 2, 4, 7 days after the therapy was started.

load changes. The results showed that only the change in viral load from day 7 to 14 was associated with the prediction of the undetectable time point ($r^2 = 0.67$). Finally, prediction in each patient was valid (Cook's D = 0.046, mean, data not shown), and we derived the following prediction formula:

Undetectable time point (week) = 13.495 × (viral load at day 14 [log IU/mL] − viral load at day 7 [log IU/mL]) + 25.456.

The degree of decrease in viral load from day 7 to 14 for the model preparation group and the actual

Table 3 Early viral dynamics of model preparation group, correlation to undetectable time point and the result of multiple linear regression analysis

	Viral load (log IU/mL)	Spearman's rank correlation test coefficient (*P*-value)	Multiple linear regression analysis r^2 (*P*-value)
Pretreatment (0 days)	5.48 ± 0.30	0.27 (0.28)	Excluded
4 h	5.66 ± 0.22	0.045 (0.82)	Excluded
8 h	5.55 ± 0.19	0.026 (0.89)	Excluded
1 day	3.74 ± 0.75	0.68 (<0.001)	Excluded
2 days	3.20 ± 0.76	0.66 (<0.001)	Excluded
4 days	4.01 ± 0.74	0.56 (0.002)	Excluded
7 days	4.05 ± 0.75	0.77 (<0.001)	Excluded
8 days	3.34 ± 0.80	0.67 (<0.001)	Excluded
14 days	3.52 ± 0.95	0.87 (<0.001)	Excluded
Subtracted values of viral load (log scale)			
1 day – 0 days	−1.78 ± 0.88	0.59 (0.001)	Excluded
2 days – 0 days	−2.18 ± 0.79	0.53 (0.003)	Excluded
4 days – 0 days	−1.46 ± 0.65	0.72 (0.000)	Excluded
7 day – 0 days	−1.38 ± 0.80	0.38 (0.049)	Excluded
14 days – 0 days	−2.24 ± 1.17	0.83 (0.000)	Excluded
2 days – 1 day	−0.55 ± 0.13	0.085 (0.67)	Excluded
4 days – 1 day	0.17 ± 0.25	0.22 (0.27)	Excluded
7 days – 1 day	0.44 ± 0.46	0.27 (0.19)	Excluded
14 days – 1 day	−0.42 ± 0.46	0.76 (<0.001)	Excluded
4 days – 2 days	0.61 ± 0.23	0.12 (0.54)	Excluded
7 days – 2 days	0.86 ± 0.50	0.12 (0.56)	Excluded
14 days – 2 days	0.11 ± 0.44	0.76 (<0.001)	Excluded
7 days – 4 days	−0.11 ± 0.17	0.047 (0.82)	Excluded
14 days – 4 days	−0.7 ± 0.37	0.78 (<0.001)	Excluded
14 days – 7 days	−0.86 ± 0.50	0.76 (<0.001)	0.667 (<0.0005)

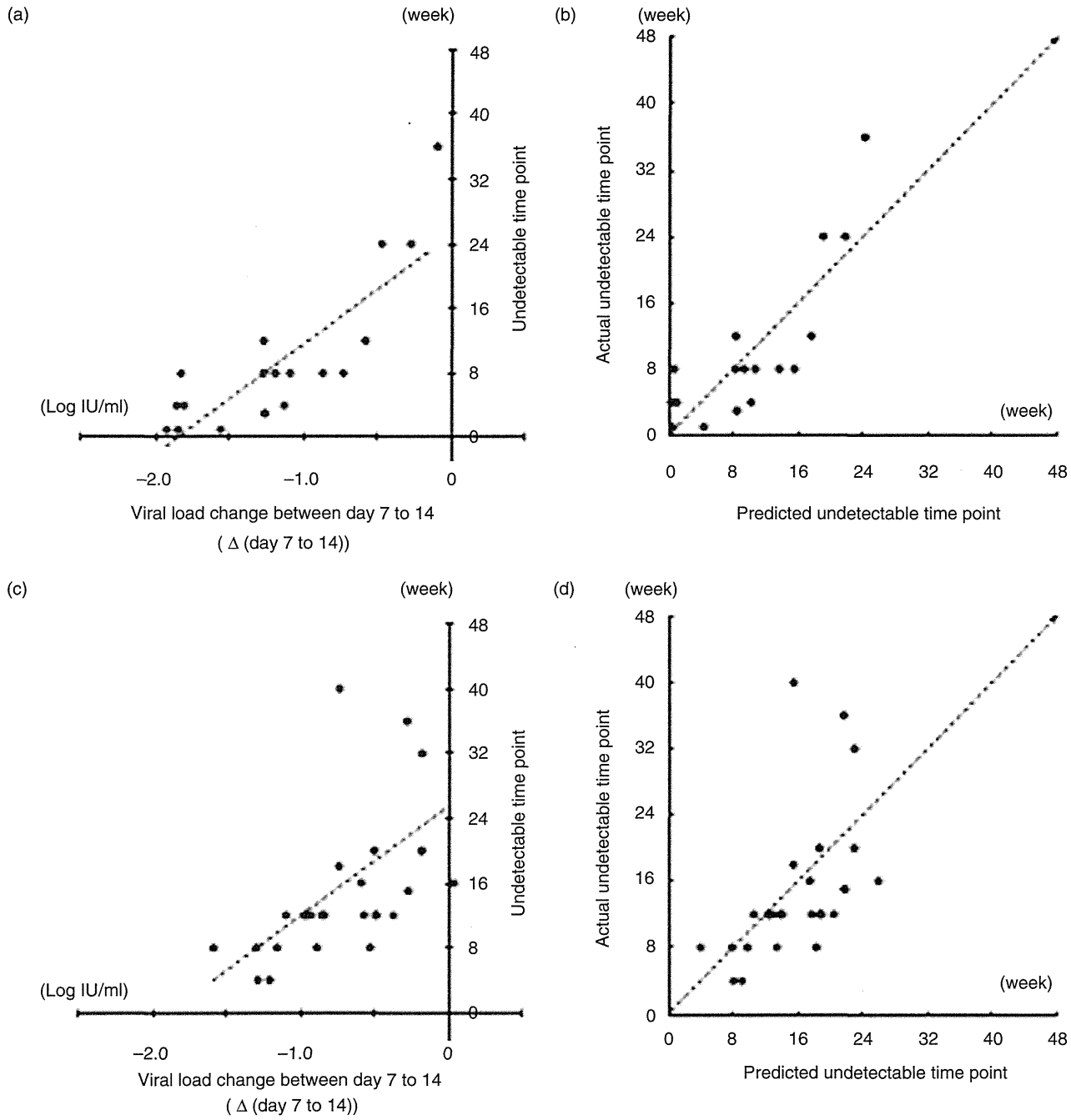

Figure 2 Correlation between the undetectable time point and the decrease in viral load from day 7 to 14 (a,b) and correlation between the actual and predicted undetectable time points (c,d). (a,c) Results of analyses for the model preparation group; and (b,d) analyses for the model validation group. Black circles, actual cases; dotted line, (a,c) estimate obtained from the prediction formula; (b,d) equal values of actual and predicted undetectable time points.

undetectable time point are plotted in Figure 2(a), which shows a very strong and a significant correlation ($r^2 = 0.67$, $P < 0.0005$).

The validity of the prediction formula was investigated in the validation group. Analysis was possible in 32 patients, as the other patients were excluded from the analysis due to the following reasons: therapy was discontinued before viral clearance in eight patients, PEG-IFN dosage was reduced before viral clearance in nine patients and viral clearance was achieved before day 14 in two patients. There were six cases of NVR, and incomplete blood collections from 13 patients on day 7 and/or 14. A strong and a significant correlation was demonstrated between the undetectable time points that were predicted using this formula and the actual undetectable time points (Fig. 2c, $r = 0.53$, $P = 0.005$).

Although only one case was predicted to achieve a rapid virological response (undetectable viral load at week 4)[13] in the model validation group, the actual undetectable time point of this patient was week 8 (Fig. 2d). In contrast, all nine cases who were predicted to achieve a complete early virological response (undetected viral load until week 12),[13] the actual undetectable time points of these patients were within week 12. Because the prediction formula was derived by the least squares method, half of the patients, who were predicted not to achieve the complete early virological response, actually achieved it.

DISCUSSION

NUMEROUS STUDIES HAVE documented that the undetectable time point is related to therapeutic responses, and its usefulness in predicting therapeutic efficacy is clear.[9–13] In the present study, we were able to derive a formula for predicting the undetectable time point for patients with HCV genotype 1b and high serum viral loads during PEG-IFN-α-2b/ribavirin combination therapy. Though the various parameters for the HCV dynamics were investigated, the change in viral load from day 7 to 14 was the only parameter that was useful for predicting the undetectable time point.

The standard length of PEG-IFN/ribavirin combination therapy is 48 weeks for patients with HCV genotype 1b and high serum viral loads; however, a 72-week administration is recommended to improve therapeutic response.[3,13,18] Therefore, when undetectable time points are predicted as from weeks 13–24 by our formula, the SVR rates could be improved by continuing the IFN therapy for longer periods. By prediction of the undetectable time point early during the treatment using our formula, the physician can make early modification and optimization of currently ongoing therapy.

Another important issue of PEG-IFN/ribavirin treatment is adherence to treatment. Because dose reductions may delay the time until serum viral clearance, patients in whom the dosage of IFN and ribavirin was reduced during therapy were excluded in the present study. However, there are many patients in whom the dosage of drugs has to be reduced during therapy for a wide variety of clinical reasons. If reducing dosage before the predicted undetectable time point, administration of IFN for longer periods should be considered.

In conclusion, we created a formula for predicting the undetectable time point in patients treated with PEG-IFN-α-2b/ribavirin combination therapy. Viral eradication is the ultimate objective of IFN-based therapy, but many patients failed to achieve viral eradication for some reason. Because our prediction formula for the undetectable time point was made with a small population, it is necessary to correct it by further analysis with a larger population. However, an early viral response reflects efficacy of the therapy, and the estimation of an undetectable time point by our formula would be useful for determining the optimal duration of treatment in the early period of the therapy for each chronic hepatitis C patient.

REFERENCES

1 Glue P, Rouzier-Panis R, Raffanel C *et al.*; The Hepatitis C Intervention Therapy Group. A dose-ranging study of pegylated interferon alfa-2b and ribavirin in chronic hepatitis C. *Hepatology* 2000; **32**: 647–53.
2 Reddy KR, Wright TL, Pockros PJ *et al.* Efficacy and safety of pegylated (40-kd) interferon alpha-2a compared with interferon alpha-2a in noncirrhotic patients with chronic hepatitis C. *Hepatology* 2001; **33**: 433–8.
3 Sánchez-Tapias JM, Diago M *et al.*; TeraViC-4 Study Group. Peginterferon-alfa2a plus ribavirin for 48 versus 72 weeks in patients with detectable hepatitis C virus RNA at week 4 of treatment. *Gastroenterology* 2006; **131**: 451–60.
4 Tsubota A, Chayama K, Ikeda K *et al.* Factors predictive of response to interferon- therapy in hepatitis C virus infection. *Hepatology* 1994; **19**: 1088–94.
5 Chayama K, Tsubota A, Kobayashi M *et al.* Pretreatment virus load and multiple amino acid substitutions in the interferon sensitivity-determining region predict the outcome of interferon treatment in patients with chronic genotype 1b hepatitis C virus infection. *Hepatology* 1997; **25**: 745–9.
6 Enomoto N, Sakuma I, Asahina Y *et al.* Mutations in the nonstructural protein 5A gene and response to interferon

in patients with chronic hepatitis C virus 1b infection. *N Engl J Med* 1996; **334**: 77–81.
7 Davis GL. Prediction of response to interferon treatment of chronic hepatitis C. *J Hepatol* 1994; **21**: 1–3.
8 Asahina Y, Izumi N, Hirayama I *et al.* Potential relevance of cytoplasmic viral sensors and related regulators involving innate immunity in antiviral response. *Gastroenterology* 2008; **134**: 1396–405.
9 Tong MJ, Blatt LM, McHutchison JG, Co RL, Conrad A. Prediction of response during interferon alfa 2b therapy in chronic hepatitis C patients using viral and biochemical characteristics: a comparison. *Hepatology* 1997; **26**: 1640–5.
10 Lee WM, Reddy KR, Tong MJ *et al.* Early hepatitis C virus-RNA responses predict interferon treatment outcomes in chronic hepatitis C. The Consensus Interferon Study Group. *Hepatology* 1998; **28**: 1411–5.
11 Davis GL, Wong JB, McHutchison JG, Manns MP, Harvey J, Albrecht J. Early virologic response to treatment with peginterferon alfa-2b plus ribavirin in patients with chronic hepatitis C. *Hepatology* 2003; **38**: 645–52.
12 Poordad F, Reddy KR, Martin P. Rapid virologic response: a new milestone in the management of chronic hepatitis C. *Clin Infect Dis* 2008; **46**: 78–84.
13 Ghany MG, Strader DB, Thomas DL, Seeff LB. Diagnosis, management, and treatment of hepatitis C: an update. *Hepatology* 2009; **49**: 1335–74.
14 Neumann AU, Lam NP, Dahari H *et al.* Hepatitis C viral dynamics in vivo and the antiviral efficacy of interferon-alpha therapy. *Scierice* 1998; **282**: 103–7.
15 Powers KA, Dixit NM, Ribeiro RM, Golia P, Talal AH, Perelson AS. Modeling viral and drug kinetics: hepatitis C virus treatment with pegylated interferon alfa-2b. *Semin Liver Dis* 2003; **23** (Suppl 1): 13–8.
16 Halfon P, Bourlière M, Pénaranda G, Khiri H, Ouzan D. Real-time PCR assays for hepatitis C virus (HCV) RNA quantitation are adequate for clinical management of patients with chronic HCV infection. *J Clin Microbiol* 2006; **44**: 2507–11.
17 Gelderblom HC, Menting S, Beld MG. Clinical performance of the new rRoche COBAS TaqMan HCV Test and High Pure System for extraction, detection and quantitation of HCV RNA in plasma and serum. *Antivir Ther* 2006; **11**: 95–103.
18 Berg T, Wagner MV, Nasser S *et al.* Extended treatment duration for hepatitis C virus type 1: comparing 48 versus 72 weeks of peginterferon-alfa-2a plus ribavirin. *Gastroenterology* 2006; **130**: 1086–97.

Clinical Study

Oncology

Oncology 2011;80:278–288
DOI: 10.1159/000328448

Received: November 9, 2010
Accepted after revision: February 23, 2011
Published online: July 7, 2011

Expression of Keratin 19 Is Related to High Recurrence of Hepatocellular Carcinoma after Radiofrequency Ablation

Kaoru Tsuchiya[a] Mina Komuta[b] Yutaka Yasui[a] Nobuharu Tamaki[a]
Takanori Hosokawa[a] Ken Ueda[a] Teiji Kuzuya[a] Jun Itakura[a]
Hiroyuki Nakanishi[a] Yuka Takahashi[a] Masayuki Kurosaki[a] Yasuhiro Asahina[a]
Nobuyuki Enomoto[c] Michiie Sakamoto[b] Namiki Izumi[a]

[a]Department of Gastroenterology and Hepatology, Musashino Red Cross Hospital, and [b]Department of Pathology, School of Medicine, Keio University, Tokyo, and [c]First Department of Internal Medicine, Yamanashi University School of Medicine, Yamanashi, Japan

Key Words
Hepatocellular carcinoma · Radiofrequency ablation · Recurrence · Keratin · Carcinogenesis · Needle biopsy · Hepatic progenitor cell

Abstract
Objective: Keratin (K) 19 positivity has been reported to be a useful predictive marker for recurrence in patients with hepatocellular carcinoma (HCC) who have undergone hepatic resection. We investigated the clinical usefulness of K19 positivity in patients who had received curative radiofrequency ablation (RFA). ***Methods:*** We retrospectively evaluated the clinicopathological features, including imaging and K19 expression, in 246 patients with HCC who were within the Milan criteria and had received curative RFA. Using a two-step insertion method, tumor biopsies were obtained just prior to RFA and were evaluated histologically. ***Results:*** Tumor seeding due to liver biopsy and RFA was not observed. Ten patients (4.1%) had K19-positive HCC. Imaging findings were similar between K19-positive and -negative HCC ($p = 0.187$). Nine out of 10 patients (90%) who had K19-positive HCC had recurrence of HCC after RFA, and intrahepatic recurrences were observed within 12 months in 6 out of 10 (60.0%). K19 positivity was a significant risk factor for recurrence ($p < 0.0001$) and early recurrence (<1 year after RFA; $p = 0.012$). K19 expression ($p = 0.016$) was an independent risk factor for tumor status exceeding the Milan criteria after RFA. ***Conclusion:*** Expression of K19 is related to high recurrence of HCC after curative RFA.

Introduction

Radiofrequency ablation (RFA) is regarded as an important treatment modality for hepatocellular carcinoma (HCC) [1–4], and its efficacy, especially for tumors <2 cm in diameter, is better than that of ethanol and nearly comparable to that of surgical resection [5]. In addition, RFA

Kaoru Tsuchiya and Mina Komuta contributed equally to this work.
Michiie Sakamoto and Namiki Izumi contributed equally to this work.

KARGER

Fax +41 61 306 12 34
E-Mail karger@karger.ch
www.karger.com

0030–2414/11/0804–0278$38.00/0

Accessible online at:
www.karger.com/ocl

Namiki Izumi, MD, PhD
Department of Gastroenterology and Hepatology
Musashino Red Cross Hospital
1-26-1 Kyonan-cho, Musashino-shi, Tokyo 180-8610 (Japan)
Tel. +81 422 32 3111, E-Mail nizumi@musashino.jrc.or.jp

is considered to be a bridge to liver transplantation because the prolonged waiting time for cadaveric livers leads to dropouts from the waiting list [6]. Tumor recurrence after curative RFA has been a problem, as it is after hepatic resection. Tumor size (>3 cm in diameter) [7], time after treatment (>1 year) [7], the number of HCC nodules [8] and hepatitis C virus (HCV) infection [8] have been reported to be risk factors for intrahepatic tumor recurrence after curative RFA. Moreover, primary technical failure is reported to be a risk factor for tumor progression beyond the Milan criteria after RFA [9].

Keratin (K) 19, which is considered to be a biliary/hepatic progenitor cell marker [10], has attracted attention as a useful predictive marker for detecting the more aggressive HCCs after curative resection, because tumors with K19 expression have a poorer prognosis [11, 12] and higher rates of recurrence [13, 14] and lymph node metastasis [12] than K19-negative HCC. In these previous studies, surgical specimens were investigated and K19 positivity was defined as expression in >5% of tumor cells [11–14].

As a result, one would expect that K19 expression might be a useful predictive marker for detecting HCC with a worse outcome after RFA, especially regarding tumor recurrence. To the best of our knowledge, the correlation between clinicopathological features and K19 expression has not been investigated in HCC patients treated by RFA. Therefore, we performed a clinicopathological study on 246 HCC cases treated with RFA and investigated the relationship between the K19 expression and recurrence and prognosis after treatment.

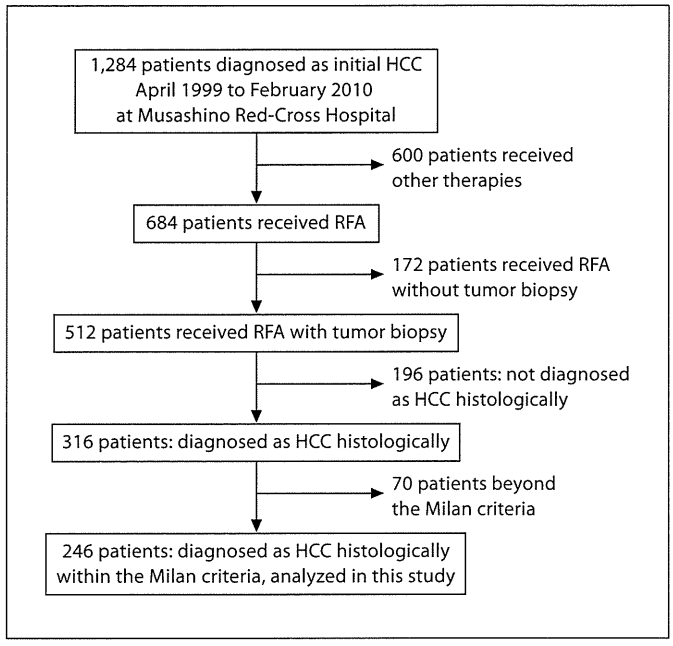

Fig. 1. Flow chart summarizing the patient selection for the study.

Methods

Patients

Between April 1999 and February 2010, 1,284 patients were admitted to the Musashino Red Cross Hospital for the first treatment of HCC. A total of 684 patients were treated with RFA as the initial therapy for HCC. Ablation therapy was chosen either because the patients were considered not to be suitable for resection (n = 323), when considering impairment of liver function, number and distribution of the tumors as well as cardiopulmonary dysfunction, or because they preferred ablation and provided informed consent (n = 361), despite surgery also being feasible. From the outset, 172 patients were excluded because RFA was performed without tumor biopsy. Therefore, 512 consecutive patients, on whom tumor biopsies had been performed before RFA, were included and we evaluated these specimens retrospectively. The result of retrospective analysis was that there were 57 patients with no residual samples, 119 patients with no tumorous lesion and 9 patients with no definitive histological diagnosis because of a small and/or fragmented specimen. The remaining specimens were diagnosed as HCC in 316 patients, as dysplastic nodule in 6 patients, as adenocarcinoma in 4 patients and as neuroendocrine tumor in 1 patient. Seventy patients were excluded, because their states of HCC were beyond the Milan criteria (≤3 cm and up to 3 nodules, or ≤5 cm and a single nodule). Therefore, 246 consecutive patients, on whom tumor biopsies had been performed before RFA and diagnosed as HCC retrospectively, were included in the study (fig. 1). The inclusion criteria for receiving RFA were as follows: total bilirubin concentration <3.0 mg/dl, platelet count $>3 \times 10^5/mm^3$, prothrombin activity >50% (approximately equal to an international normalized ratio of 1.5) and Child-Pugh score <8 points. Ascites were controlled by administration of diuretics before RFA. Patients with macroscopic vascular invasion or extrahepatic metastases were excluded. The criteria of the International Union against Cancer were used for TNM classification [15]. Written informed consent was obtained from all patients, and the study was approved by the ethics committee at Musashino Red Cross Hospital, in accordance with the Declaration of Helsinki.

Diagnosis of HCC

All the patients were diagnosed as having HCC on the basis of tumor markers and a combination of typical imaging findings on ultrasonography (US) and dynamic computed tomography (CT), according to the American Association for the Study of Liver Diseases and the Japan Society of Hepatology guidelines [1, 16]. When patients had 2 or 3 HCC nodules, a needle biopsy was taken from the main nodule. The histological diagnosis of HCC was based on the World Health Organization criteria [17].

For the evaluation of vascularity and Kupffer cell activity of the target nodule, CT during arteriography (CTHA) and CT dur-

ing arterioportography (CTAP) were performed in 188 (76.4%) patients, superparamagnetic iron oxide-enhanced magnetic resonance imaging (SPIO-MRI) was performed in 194 (78.8%) patients and gadolinium-ethoxybenzyl-diethylenetriamine pentaacetic acid magnetic resonance imaging (Gd-EOB-DTPA) was performed in 47 patients (19.1%), from March 2008. For triple-phase dynamic CT scans, arterial, portal and equivalent phases were 35, 70 and 150 s, respectively, after injection of contrast agent. Spiral CT scans were obtained from 3- to 5-mm-thick sections. Board-certified radiologists diagnosed HCC on the basis of typical patterns, such as an early-phase hyperattenuation area and late-phase hypoattenuation on dynamic CT. According to previous studies, the sensitivity of the diagnosis of HCC in CTHA/CTAP is higher than that of spiral CT. The diagnosis of HCC in CTHA/CTAP is hyperattenuation area in CTHA and hypoattenuation area in CTAP. It has been reported that the presence of Kupffer cells could be evaluated, and this was defined by a hyper-intensity area in the T2* image of SPIO-MRI as a typical imaging finding of HCC. Gd-EOB-DTPA MRI is a liver-specific contrast-enhanced agent, and hypointensity in the hepatobilliary phase is a typical imaging finding. We started to perform Gd-EOB-DTPA MRI instead of SPIO-MRI from March 2008, because it was reported that the sensitivity of Gd-EOB-DTPA MRI was superior to SPIO-MRI for the diagnosis of HCC.

Tumor Biopsy and RFA

There are 24 operators who participated in this study. They are specialized liver physicians who have great experiences in performing percutaneous ethanol injection for HCC, percutaneous tumor biopsy for liver tumor, percutaneous liver biopsy for hepatitis, percutaneous hepatobiliary drainage for obstructive jaundice, or percutaneous liver abscess drainage. A needle-guiding technique was used, consisting of an initial guided needle and a secondary outer needle (two-step insertion method). This method was reported by another center previously [18] and involves the initial insertion of a 21-gauge needle (Silux, Saitama, Japan) just adjacent to the tumor under real-time US guidance, and using this to insert a 14-gauge Daimon outer needle (Silux), also just adjacent to the tumor. After removal of the inner needle, an 18-gauge biopsy needle was inserted to obtain the tumor tissue sample. After removal of the biopsy needle, a 17-gauge cooled-tip electrode was inserted into the targeted tumor. The electrode, with a 2- or 3-cm exposed tip, was connected to a 480-kHz RF Generator (Radionics, Burlington, Mass., USA), which produces 200 W at 50 Ω of impedance [19, 20]. The equipment also allows the measurement of power output, tissue impedance and electrode tip temperature. A tip temperature of 10–20°C was maintained by infusion of chilled water through a peristaltic pump. After insertion of the electrode into the tumor, ablation was performed at 60 W for the 3-cm exposed tip and 40 W for the 2-cm exposed tip. The power was increased to 140 W at a rate of 10–20 W/min. When a rapid increase in impedance was observed during thermal ablation, the output was reduced. The duration of a single ablation was 12 min. After RF exposure, the pump was stopped and the temperature of the needle tip was measured. When the temperature of the electrode tip was >60°C, ablation was defined as being sufficient. When the target nodule was >2 cm in diameter, multiple needle insertions and ablations were performed in 1 nodule to achieve complete necrosis. A session was defined as a single intervention consisting of ≥1 ablations performed on ≥1 tumors at the same time. After completion of nodule ablation, the intrahepatic needle track was treated by thermocoagulation to avoid needle track seeding. Finally, a mixture of gelatin sponge particles (Gelfoam®; Upjohn, Kalamazoo, Mich., USA) was injected into the puncture route. All procedures were completed within 15–20 min. After each session of RFA, a dynamic CT scan (section thickness 5 mm) was performed to evaluate the efficacy of ablation. Complete ablation of HCC was defined as non-enhancement of the lesion, including the whole surrounding liver parenchyma. The ablative margin was shown as the boundary between the low density area as ablated area and the isodensity area as surrounding normal liver parenchyma. The residual portion of the tumor was treated by additional RFA within a few days of the post-treatment CT scan. Follow-up consisted of monthly serial measurements of tumor markers [α-fetoprotein (AFP) and des-γ-carboxy prothrombin (DCP)], US examination every 2 months and dynamic CT every 3 months. We checked various complications of RFA with conventional contrast-enhanced CT and blood examination at day 1 after RFA.

Tumor Recurrence

Recurrence of HCC was defined as an early enhancement area on dynamic CT, concomitant with late wash out. Two types of recurrence, local tumor progression and distant intrahepatic recurrence, were identified. Local tumor progression was defined as an enhancing area located adjacent to the ablated area [21], while distant intrahepatic recurrence referred to the appearance of a new tumor in the liver, distant from the ablated area. Early recurrence was defined as a recurrence within 12 months of the initial RFA.

Immunohistochemistry

Immunohistochemistry using antibodies against K19 (1:100, BA17, Dakocytomation, Glostrup, Denmark) was performed on paraffin-embedded sections from 246 needle biopsy specimens. The slides were reviewed by 2 independent pathologists (M. Komuta and M. Sakamoto). Expression of K19 was considered positive if >5% of tumor cells were stained according to the expected pattern of reactivity.

Statistical Analysis

Categorial variables were compared with the χ^2 test and continuous variables with the Mann-Whitney test; a p value <0.05 was considered statically significant. Continuous variables were expressed as the mean ± standard deviation. The imaging findings were compared with the χ^2 test between K19-positive and -negative patients. Overall survival was defined as the interval between treatment and death or the date of the last follow-up or the date of the most recent follow-up visit. Probability of recurrence-free survival was defined as the interval between treatment and the date of HCC recurrence.

Univariate analysis was performed to identify clinical and biological parameters (sex, age, etiology, prothorombin activity, albumin, bilirubin levels, Child-Pugh class, serum AFP level, serum DCP level) and tumor factors (size, number, tumor stage, tumor differentiation, K19 expression) predicting overall survival, recurrence-free survival and the interval beyond the Milan criteria.

Survival curves were computed according to the Kaplan-Meier method and compared by the log-rank test. All variables with a p value <0.05 were subjected to multivariate analysis by Cox's

Table 1. Comparison of clinicopathological features of patients (n = 246) with HCC with and without K19 expression

Features	K19 >5% (n = 10)	K19 ≤5% (n = 236)	p value
Mean age ± SD, years	70 ± 8	68 ± 8	0.541
Sex, male/female	2/8	146/90	0.016
Clinical and laboratory data			
Mean AFP, ng/ml	489 [52.1]	12 [16.2]	0.062
Mean DCP, mAU/ml	42 [25]	321 [22]	0.773
Child-Pugh score A/B	8/2	200/36	0.655
Total bilirubin, mg/dl	0.9 ± 0.5	0.8 ± 0.4	0.480
Albumin, g/dl	3.4 ± 0.7	3.6 ± 0.5	0.137
PT, %	97 ± 12	92 ± 15	0.375
Pathology			
Tumor size, mm	24 ± 7	22 ± 8	0.392
Tumor number	1.3 ± 0.7	1.2 ± 0.6	0.891
Vascular invasion, yes/no	0/10	0/236	
Tumor differentiation well/moderate/poor	0/8/2	108/126/2	<0.0001
TNM stage I/II	8/2	183/53	0.855
Lymph node involvement yes/no	0/10	0/236	
Metastasis, yes/no	0/10	0/236	
Major associated liver diseases			
HBsAg+	1 (10)	24 (10.1)	0.895
HCV Ab+	9 (90)	189 (80.1)	
ALD	0	8 (3.4)	
NASH	0	2 (0.8)	
Unknown etiology	0	13 (5.6)	

Figures in parentheses are percentages; figures in brackets are medians. PT = Prothrombin time; HBsAg = hepatitis B surface antigen; HCV Ab = HCV antibody; ALD = alcoholic liver disease; NASH = non-alcoholic steatohepatitis.

Table 2. Comparison of the image findings of patients with HCC with and without K19 expression

	K19 positive >5% (n = 10)	K19 negative (n = 236)	p value
CECT arterial phase high density	10/10	200/235	0.187
CTHA high density	7/7	159/181	0.326
CTAP low density	7/7	179/181	0.779
SPIO-MRI T2*	10/10	175/184	0.473
EOB-MRI			
Hepatobiliary phase low intensity	–	46/47	–

proportional hazards model to assess their value as independent predictors.

All statistical analyses were performed using StatView (version 5.0) software (Abacus Concepts, Berkeley, Calif., USA).

Results

Proportion of HCCs Expressing K19

The biopsy number was 272, and the median length of our biopsy specimens was 8.2 ± 4.0 mm. In 117 cases, the specimens were <1 cm, and ≥1 cm in 155 cases. Pathological diagnosis and K19 staining were practicable in all specimens <1 cm. Expression of K19 in >5% of tumor cells was observed in HCCs from 10 of 246 patients (4.1%). Two of the 10 HCCs (20.0%) were poorly differentiated, and 8 (80.0%) were moderately differentiated. None of the well-differentiated HCCs showed K19 positivity. Among the 10 patients with K19-positive HCCs, 2 had a HCC nodule >3 cm and 8 had HCC nodules ≤3 cm in diameter. The 8 HCC nodules with K19 positivity ≤3 cm in diameter were moderately (n = 7) and poorly differentiated HCCs (n = 1).

Clinicopathological Characteristics of Patients with HCC in Relation to Expression of K19

The clinicopathological characteristics of the patients in relation to K19 expression in HCCs are shown in table 1. The proportion of well-differentiated HCCs was significantly lower among K19-positive HCC patients ($p < 0.0001$). K19 expression was more frequent among female than among male patients ($p = 0.016$). There were no significant differences in age, clinical laboratory data, tumor size, number of tumor nodules, tumor stage in TNM classification or etiology between K19-positive and -negative HCC patients. There was no significant difference in tumor location (near the major vessels, bile ducts and organs) between K19-positive and -negative patients. The number of RFA sessions did not differ significantly between K19-positive and -negative HCC patients. Serum AFP before initial RFA was not evaluated in 1 patient.

Imaging Characteristics of HCCs in Relation to Expression of K19

Comparison of the various imaging findings, according to vascular profiling, and in relation to K19 expres-

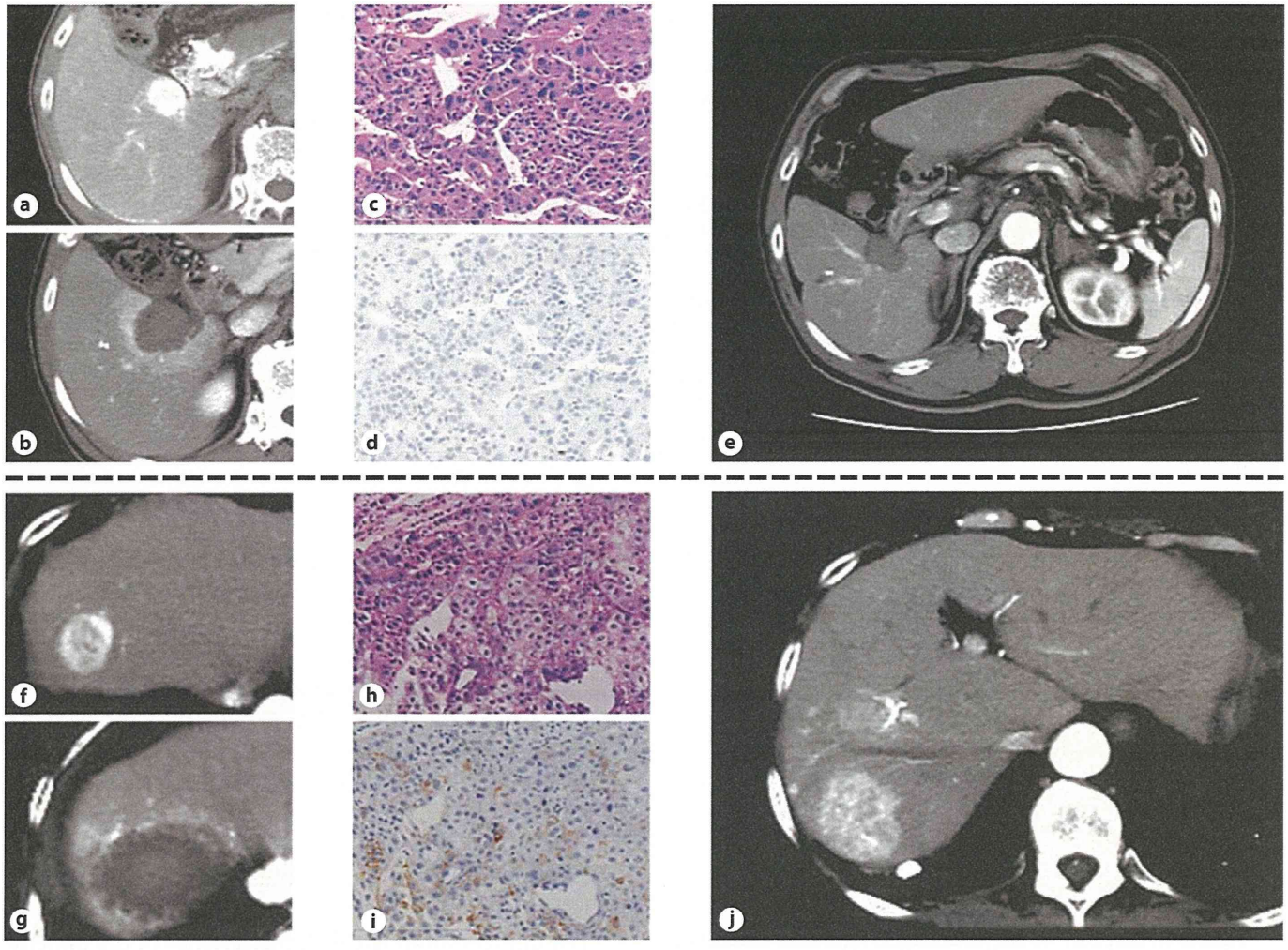

Fig. 2. a–e A patient with K19-negative HCC: a 70-year-old man with chronic hepatitis (anti-HCV positive). The HCC (25 mm in diameter, in segment 6) showed an early enhancement area by dynamic CT (**a**). Dynamic CT at 1 day after RFA (**b**). On histological investigation, the tumor showed moderately differentiated HCC on H&E staining (**c**), and K19 expression was negative in tumor cells (**d**). The HCC did not show early enhancement on dynamic CT 4 years and 10 months after curative RFA (**e**). **f–j** A patient with K19-positive HCC: a 72-year-old female with chronic hepatitis (anti-HCV positive). The HCC (25 mm in diameter, in segment 8) showed an early enhancement area by dynamic CT (**f**). CT 1 day after RFA (**g**). On histological investigation, the tumor showed moderately differentiated HCC on H&E staining (**h**), and K19-positive cells were seen in the tumor (**i**). Five months after RFA, the HCC showed intrahepatic recurrence beyond the Milan criteria (**j**).

sion, is shown in table 2. These imaging findings were consistent with the histological diagnosis, as determined by pretreatment needle biopsy.

All K19-positive HCCs showed typical HCC images, such as hypervascularity at the arterial phase, hypovascularity at the portal and equilibrium phases in dynamic CT, and hyperintensity at the T2* image in SPIO-MRI. There was no significant difference between K19-positive and -negative patients in terms of the imaging findings.

Recurrence of HCC after RFA

The median follow-up period was 34.0 months (range 65 days to 10.3 years). A recurrence of HCC was diagnosed at least once during the follow-up period in 156 patients (63.4%). The cumulative recurrence-free survival at 1, 3 and 5 years was 69.9, 26.6 and 12.2%, respectively. Among the 156 patients with recurrent HCC, 14 (8.9%) had local tumor progression and 142 (91.1%) had distant intrahepatic recurrences. Five of 14 patients (35%) who had local tumor progression had K19-positive HCC and